Chemically and Mechanically Controlled Single-Molecule Switches using Spiropyrans

Mark C. Walkey,[†a] Chandramalika R. Peiris,[†b] Simone Ciampi,[b] Albert C. Aragonès,[c] Ruth B. Domínguez-Espíndola,[b] David Jago,[a] Thea Pulbrook,[a] Brian W. Skelton,[a] Alexandre N. Sobolev,[a,d] Ismael Díez Pérez,[c] Matthew J. Piggott,[a] George A. Koutsantonis[a]* and Nadim Darwish[b]**

[a]Chemistry, M310, School of Molecular Sciences, The University of Western Australia, Perth, WA 6009, Australia

[b]School of Molecular Science and Curtin Institute of Functional Molecules and Interfaces, Curtin University, Bentley, WA 6102, Australia

[c] Department of Chemistry, Faculty of Natural & Mathematical Sciences, King's College London, Britannia House, 7 Trinity Street, London SE1 1DB, United Kingdom

[d] Centre for Microscopy, Characterisation and Analysis, The University of Western Australia, Perth, WA 6009, Australia

E-mail: nadim.darwish@curtin.edu.au; matthew.piggott@uwa.edu.au; george.koutsantonis@uwa.edu.au

† These authors contributed equally

KEYWORDS: (single-molecule switches, mechano-electronic switches, chemo-electronic switches, single-molecule electronics, molecular electronics)

ABSTRACT: Developing molecular circuits that can function as the active components in electrical devices is an ongoing challenge in molecular electronics. It demands mechanical stability of the single-molecule circuit while simultaneously being responsive to external stimuli mimicking the operation of conventional electronic components. Here, we report single-molecule circuits based on spiropyran derivatives that respond electrically to chemical and mechanical stimuli. The merocyanine that results from protonation/ring-opening of the spiropyran form showed single-molecule diode characteristics, with an average current rectification ratio of 5 at ± 1 V, favouring the orientation where the positively charged end of the molecule is attached to the negative terminal of the circuit. Mechanical pulling of a single spiropyran molecule drives a switch to a more conducting merocyanine state. The mechanical switching is enabled by strong Au–C covalent bonding between the molecule and the electrodes, which allows the tensile force delivered by the STM piezo to break the molecule at its spiropyran C–O bond.

1. INTRODUCTION

The goals of molecular electronics have progressed beyond the need for simple molecular conductors and thus the need to develop switches, transistors and diodes has become paramount.[1-5] Molecular junctions mimicking solid-state transistors and diodes have been addressed using light, pH and electrochemical potential using a wide range of molecules.[6-14] To date, most of these molecular circuits respond to a specific stimuli or have a limited change in their structure upon exposure to a stimulus, which limits their applications in nano-circuitry.

We have recently introduced spiropyran derivatives as active components in single-molecule electrical circuity.[8] The advantages of spiropyrans, over other switching molecules, include the large range of stimuli that are able to induce their reversible isomerization: light, changes of the solvent, metal ions, gases, acids and bases, force and temperature.[15-18]These properties are promising for developing single-molecule electrical devices in which conductance can be controlled by multiple external stimuli, offering potential applications in nanoscale logic gates. The isomerization of a ring-closed spiropyran (SP) to its zwitterionic merocyanine (MC) ring-open state can be used for the fabrication of molecular diodes, switches and as mechanically responsive circuits as we explain below.

Spiropyrans are usually colorless, UV-light absorbing molecules consisting of indoline and chromene ring systems, oriented almost orthogonal to one another, and linked through a common spiro carbon (Scheme 1).[16] In the **SP** form, electronic conjugation between the two heterocycles is absent. A range of external stimuli cause ring-opening to give a coloured **MC** form that has more conjugation between the chromene and the indoline portions of the molecule and therefore has higher conductance. The chemical transformation between the closed and open state is initiated by the cleavage of the spiro C–O bond, which results in an twisted ***cis*-MC**, which isomerises to the largely planar ***trans*-MC**.[16]

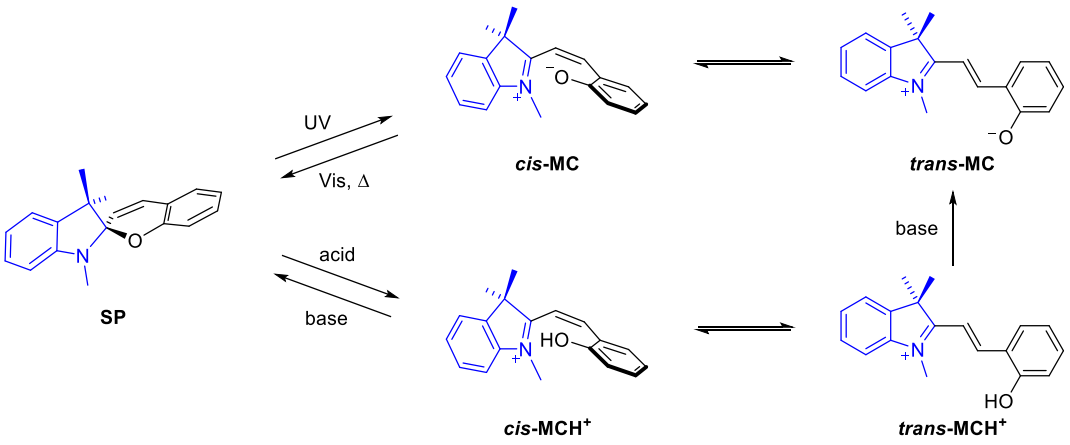

Scheme 1. The parent spiropyran (**SP**) molecule, with the indolene and chromene moieties represented in blue and black, respectively, linked by the central spiro carbon atom. Ring-opening is induced by UV light or acid to give the merocyanine (**MC**), or protonated merocyanine (**MCH**$^+$), respectively. Ring-closure occurs thermally and is generally accelerated by visible light.

The ***cis*-MC** state resembles a strong electron donor–acceptor combination separated by a π-bridge that has a nonplanar structure and therefore poor orbital overlap between the electron donor (–O$^-$) and acceptor (=N$^+$) (Figure 1). This donor–twisted bridge–acceptor state resembles a molecular diode, similar to that proposed by the original report of Aviram and Ratner.[19] If captured between two electrodes, the merocyanine molecule should favour the passage of electric current from the electron acceptor to the donor. Depending on the dihedral angle about the central C=C bond, which can be modulated in molecular junctions, the degree of orbital overlap between the electron donor and the acceptor can be controlled. The merocyanine is therefore potentially a tunable molecular diode.

One of the stimuli that can trigger the isomerization of spiropyran to merocyanine is mechanical force, which can be achieved by physically pulling the ends of the molecule to break the C–O bond of the spiro center. For example, application of tensile stress to glassy polymers containing embedded spiropyrans caused ring-opening to the merocyanine state, as evinced by color change.[20] For mechanical stress-induced switching to be successful in single-molecule junctions, robust anchors (A) to the electrodes are required such that the contact

bonds are stronger than, or at least comparable to, the spiro C–O bond that undergoes mechanically rupture (Figure 1b). The bond dissociation energy of the spiro C–O bond is in the range of 30–50 Kcal/mol.[21]

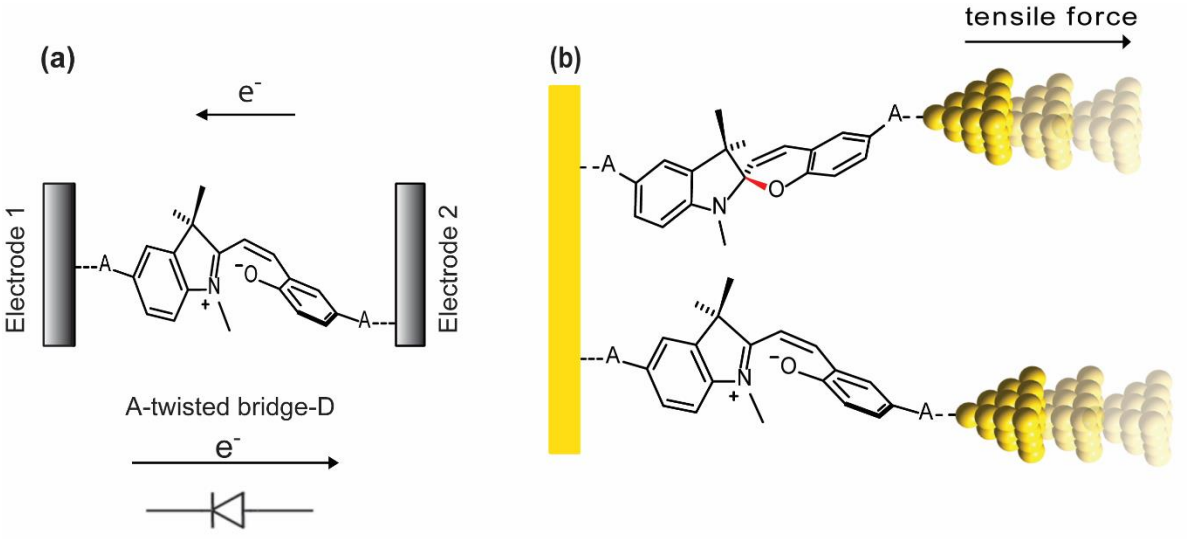

Figure 1. (a) Schematic describing the operation of a molecular diode using the open merocyanine molecule. Current would be expected to flow efficiently from −ve terminal---acceptor---donor---+ve terminal. The degree of conjugation between the donor and acceptor will dictate the degree of current rectification. (b) Schematic describing the operation of a mechano-responsive switch. The C–O bond in red is expected to break if the bond dissociation energies of the molecule–electrode contacts are higher than that of the C–O.

Other compounds with a spiro centre that were previously used in molecular junctions contained weak anchor groups such as $–NO_2$ or –CN.[8] Despite their weak affinity to gold electrodes, the $–NO_2$ and –CN terminated spiropyrans have demonstrated conductance switching of an order of magnitude under UV light and acid stimuli.[8] However, due to the short life-time of the single-molecule junctions, it was not possible to investigate the current–voltage properties of these junctions as the contacts are not capable of withstanding the high electric fields imposed during voltage ramping. Similarly, the response to mechanical stimuli could not be investigated as the gold–molecule contacts cleaved under mechanical stress.

Herein, we describe the synthesis, characterisation, surface assembly and single-molecule conductance measurements of two spiropyrans terminated with pyridyl and alkynyl groups

using scanning tunnelling microscopy break-junction approaches (STM-BJ). The anchor groups were chosen such that strong molecule–electrode contacts would be formed, resulting in long junction lifetimes and enabling the study of molecular switching in-junction under ambient conditions. Single-molecule conductance switching, current–voltage properties at the single molecule level, and response to tensile strain were investigated.

2. RESULTS AND DISCUSSION

2.1. Design, synthesis and characterization

The symmetrical functionalization of a spiropyran molecule by electrode-anchoring groups is necessary for a single-molecule junction study. Pyridyl groups are commonly used as the contacts for single molecule junctions between gold electrodes, while terminal alkynes are less explored but have recently been suggested to spontaneously form strong covalent bonds to gold electrodes.[22] The sp-C–Au bonds are much stronger than S–Au or N–Au bonds formed with thiol and pyridyl anchor groups, respectively, enabling long junction lifetime previously inaccessible for single molecules.[22] We therefore sought to design, synthesise and compare the electrical properties of single spiropyran molecules terminated at both ends with pyridyl or ethynyl groups, and test the suitability of these different contacts for different stimuli-triggered switching.

The spiropyran targets were prepared by initial condensation[23-24] of the indolium iodide **1**,[25] and the ethynyl substituted salicylaldehyde **2**,[19] which provided **3** (Scheme 2). Deprotection afforded the terminal alkyne **SP-1**, which underwent Sonogashira coupling[26] with 4-iodopyridine to give the pyridyl terminated **SP-2**. Full characterization of compounds **3**, **SP-1** and **SP-2** can be found in section 1 and Figures S1−S6 of the Supporting Information. The structures of **3** and **SP-1** were confirmed by X-ray crystallography (Figures S7, S8 and Table S1, Supporting Information).

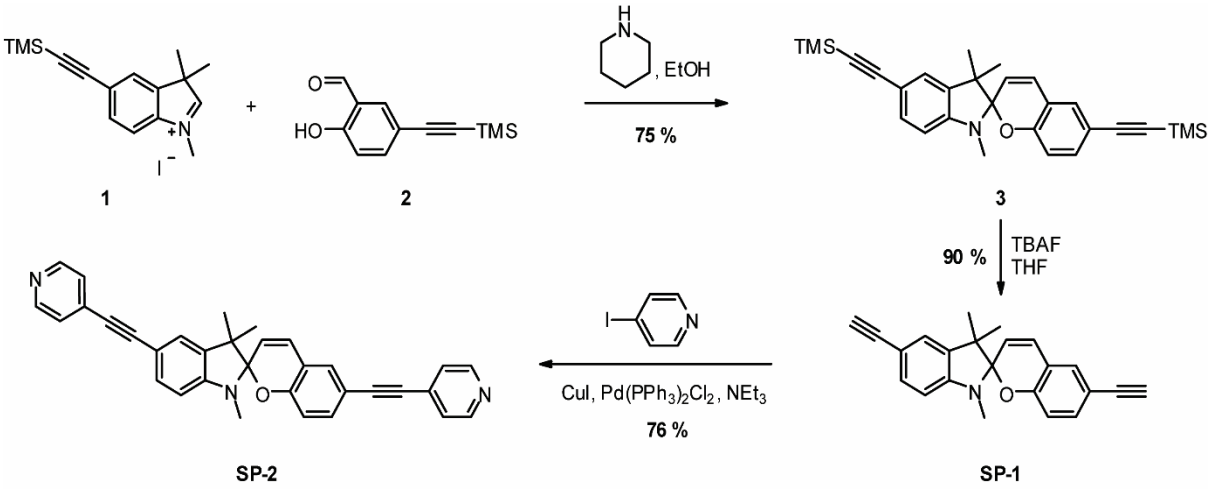

Scheme 2. Synthesis of the targeted spiropyrans.

2.2. Bulk Characterization

For the purpose of testing the ability of **SP-1** to form stable and spontaneous contacts to gold electrodes, we formed self-assembled monolayers (SAM) using **SP-1** on Au (111) electrodes. The results from XPS measurements on SAMs of **SP-1** on Au (111) are provided in Figure S9 of the Supporting Information. The presence of C–C at 284.65 eV, C–N and C–O at 286.15 eV, O–C–N at 287.65 eV and N 1s at 399.54 eV support the formation of a monolayer of **SP-1**. The presence of alkyne moieties on the distal end of the monolayer was confirmed by the successful attachment of azidomethylferrocene (Fc) via 'click' alkyne-azide copper-catalysed reactions. Figure 2 shows the Fc electrochemical signal of the resulting surface reaction with an estimated Fc coverage between 3.7 x 10^{-11} and 6.7 x 10^{-11} mol cm^{-2}. This translates to about 10-20 % of a full coverage-limit of a tightly packed ferrocene terminated monolayer of alkanethiols on gold.[27-28] This coverage is lower than that reported for click reactions of ferrocene on terminal alkynes via nonadiyne monolayers (30-50%)[29] which can be explained by a partial hairpin-assembly where some molecules are positioned flat with both alkynes forming a bond with surface. The waves of the cyclic voltammetry were relatively stable but

with a considerable decrease in the current response after continuous cycling which is ascribed to the loss of the ferrocene during voltammetry[30] as opposed to the desorption of the **SP-1** monolayer itself (Figure S10, Supporting Information).

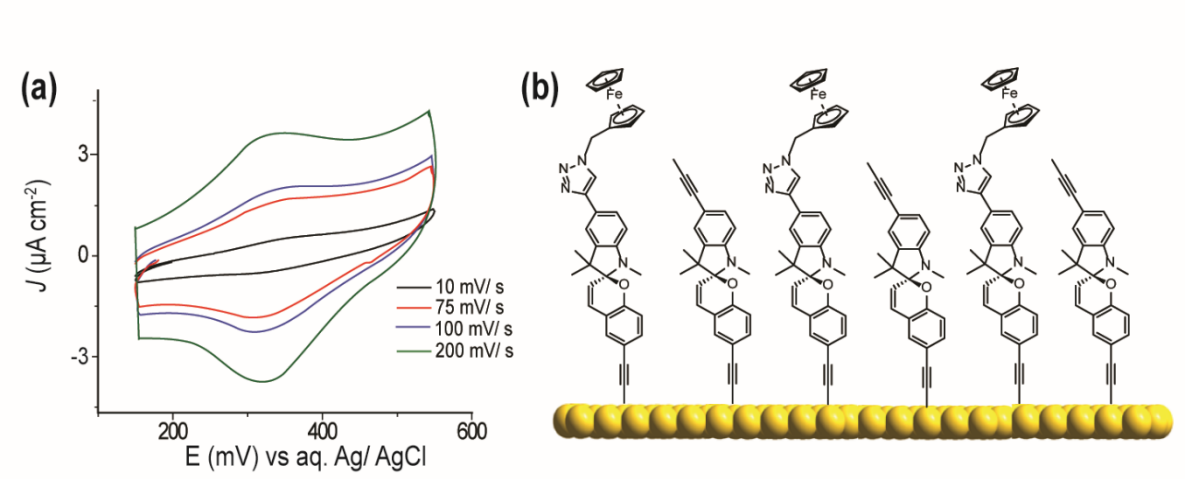

Figure 2. (a) Cyclic voltammetry at different scan rates for **SP-1** terminated with a clicked ferrocene moiety on an Au (111) electrode. The current density increases linearly with scan rate, indicating a surface redox reaction. The voltammograms were recorded in 0.1 M $NaClO_4$ and the potential is expressed in mV against aq. Ag/AgCl electrode (1 M KCl). (b) A schematic describing the surface chemistry: a monolayer of **SP-1** is assembled on Au (111) followed by the attachment of azidomethylferrocene (Fc) via a 'click' alkyne–azide copper-catalysed cycloaddition reaction. Only one possible surface orientation of **SP-1** is depicted in Figure 2b. For the click reaction, the **SP-1**-functionalized Au (111) surface was exposed to (i) azidomethyl-ferrocene (10 mM, ethanol/water, 2:1), (ii) copper(II) sulfate pentahydrate (0.8 mol% relative to the azide) and iii) sodium ascorbate (80 mol% relative to the azide).

When **SP-2** and **SP -1** are irradiated with UV light there is no detectable MC optical absorption (ca. 600 nm). This is likely due to rapid thermal reversion of the MC to the SP form. In fact, both **SP-1** and **SP-2** do not contain the electron withdrawing NO_2 group, usually required in UV-switchable spiropyrans, at the chromene side of the molecules[16]. The absence of the electron withdrawing group makes the phenoxide anion ($-O^-$) of the open MC state highly nucleophilic and consequently induces a significantly faster cyclization of MC back to SP. However, upon the addition of trifluoroacetic acid (TFA), **SP-2** was found to switch rapidly to the open protonated merocyanine state **MCH$^+$-2**, leading to a yellow solution with an absorption maximum at 415 nm. In contrast to the MC formed by photo-switching, protonation of the phenolic oxygen in **MCH$^+$-2** prevents thermal ring-closure, resulting in quantitative

conversion of **SP-2** to the open form. The protonation/ring-opening sequence is fully reversible, as evident from the restoration of the UV-Vis absorption peak for **SP-2** upon neutralization of **MCH$^+$-2** with triethylamine (TEA) (Figure 3c and Figure S11, Supporting Information). The same case was not observed for **SP-1** and only limited switching to the **MC-H$^+$-1** (420-500 nm) was observed upon the addition of acid even after adding several equivalents of the acid (Figure S11, Supporting Information). The reason why **SP-1** does not switch as neatly and reversibly in acid/base as **SP-2** could possibly be due to the acid protonating the -N$^+$ in the core of the **SP-1**[31] which makes a complete shift of equilibrium towards the **MC-H$^+$-1** not possible.

2.3. Single-molecule measurements

2.3.1. Acid/base conductance switching

Single-molecule circuits of **SP-2** between two gold electrodes (Figure 3a) were first formed using the STM-BJ technique via the "tapping" or current -stretching approach.[32-33] The method is based on forcing a freshly prepared gold STM tip in and out of contact with a gold substrate in the presence of a dilute solution of **SP-2**. During the contact, pyridyl anchored molecules can bridge the tip and the surface electrodes. As the STM tip is pulled away from the surface, plateaus appear in the current versus distance traces (Figure 3b), which are attributed to single-molecule events. It is important to note the shape of these current plateaus reflects the evolution of the current passing through the molecule while the molecule is mechanically stretched. As shown in Figure 3b, most of the current plateaus for **SP-2** are either flat or only slightly changed during stretching. This is observed for most molecular junctions since only limited change in the structure of typical organic molecules can happen during stretching. The plateau length is also considerably less than the molecular length of **SP-2**, indicating that the junction breaks before a full stretch of the molecule. The limited change in current during the lifetime of the

SP-2 plateaus is expected if all bonds within the molecule remains intact during the stretching process. We conclude therefore that **SP-2** remains in its closed spiro form upon stretching and that the spiro C–O bond remains intact during stretching. We attribute this to the C–O bond being stronger than that of pyridine–gold contacts. Hence, the molecular junctions would likely break from their contact points with the electrodes before sufficient strain to break the spiro C–O bond can be applied. The absence of switching during stretching **SP-2** junctions can, however, be used as an advantage in studying acid/base switching since any changes in the conductivity can be exclusively related to the external stimulus and not those induced by molecular strain. A statistical value of the single-molecule conductance was obtained by accumulating thousands of current–distance traces into conductance histograms (Figure 3d), with a conductance magnitude of 2.25×10^{-5} G_0 (1 G_0= 77.5 μS) obtained for **SP-2**.

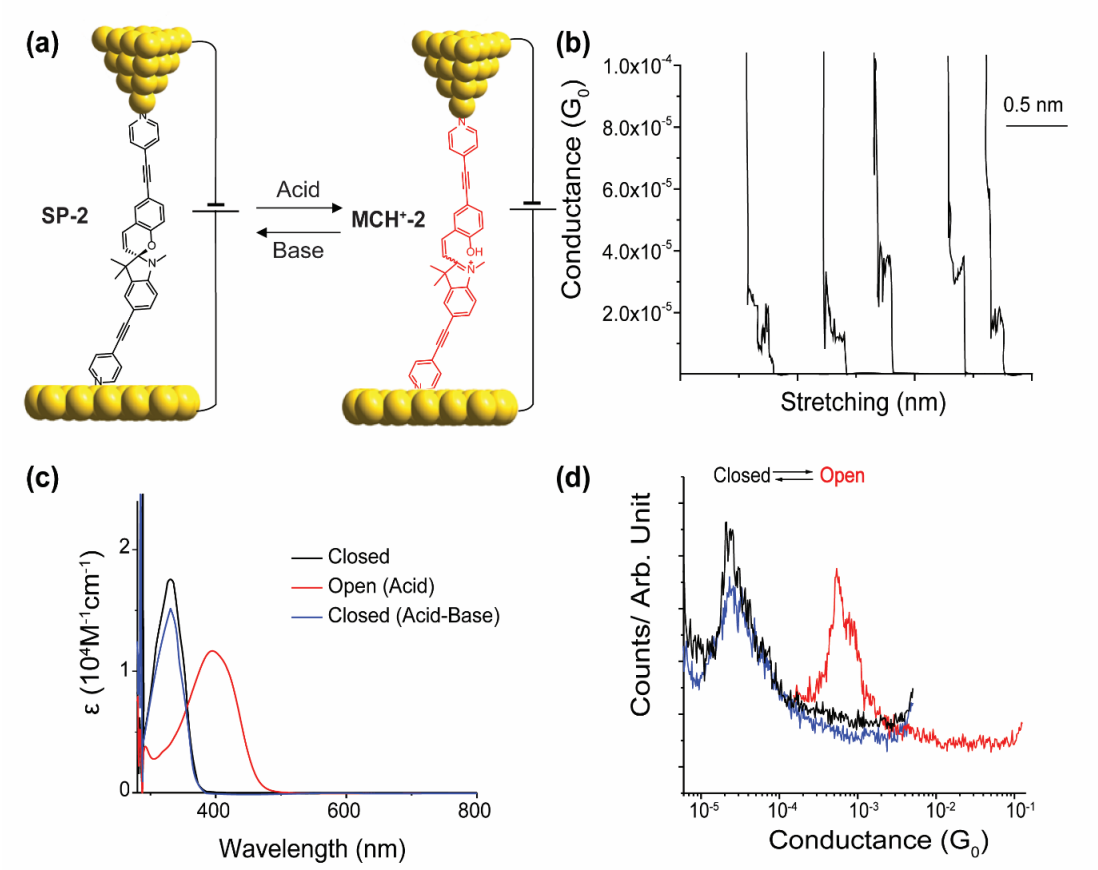

Figure 3. (a) Schematic describing the acid-base switching of **SP-2** to the protonated merocyanine **MCH$^+$-2.** (b) Representative STM-BJ current–distance curves of **SP-2**. Current–distance curves for **MCH$^+$-2** samples is shown in Figure S12 of the Supporting Information. (c) UV-Vis absorption spectra of **SP-2** solutions in dark (black line), after the addition of an organic acid (TFA, red line), and after the addition of the neutralizing base (TEA, blue

line). (d) STM-BJ conductance histograms for dark **SP-2** samples (black line), samples after the addition of TFA (red line) and after the addition of TEA (blue line). The conductance histograms were obtained at a bias voltage of 25 mV.

Upon the addition of TFA, the single-molecule conductance of **SP-2** switches to a higher conductance value of 5.7×10^{-4} G_0, about 25-fold higher than that of the closed state (Figure 3d, red data). This high conductance state is assigned to the open and protonated **MCH$^+$-2** state. The higher conductivity of the **MCH$^+$-2** states is likely due to a HOMO-LUMO gap that is smaller than that of the **SP-2** form. The smaller band gap would bring one of the frontier orbitals closer to the gold Fermi level increasing the conductivity. The change in conductance was completely reversible by the addition of TEA (Figure 3d, blue data) and can be performed for at least two complete cycles (Figure S13, Supporting Information). It is worth noting that a switch from the **SP** to the **MC** state can be possibly induced by a high bias voltages and therefore high electric field.[34] However, at biases above 500 mV the junctions become relatively unstable and any attempt to quantify electric field induced isomerization was not attempted in these systems.

2.3.2. Current–Voltage properties of SP-2

In addition to the current-distance (tapping) method above, we have performed current-time measurements referred to as the "blinking" or the "I(t)" method[35] on **SP-2** adopted from the pioneering work of Nichols and co-workers.[36-37] In the blinking method, the STM tip and the surface are fixed in position. When a molecule bridges the gap between the electrodes, an increase in the current above the background tunnelling current (tunnelling through the gap space) is observed. This is reflected in sudden jumps in the monitored current in the form of telegraphic signatures or ''blinks'' (Figure 4a). The current then drops back to the through-space tunnelling current after the junction breaks. Representative blinks of **SP-2** and **MCH$^+$-2** are shown in Figure S14 of the Supporting Information. The importance of this method is that

it enables a long-life time sufficient to ramp the voltage and measure the current-voltage properties of the single-molecule junctions (Figure 4b). This enables *in-situ* monitoring of the effect of external stimuli (e.g. voltage ramping) on the current. The single-molecule conductance in the blinking method was found to be comparable to that of the tapping method with values of 2.50×10^{-5} G_0 and 6.0×10^{-4} G_0 for the **SP-2** and **MCH$^+$-2** states, respectively.

The average lifetime of the blinks were ca. 0.5 s for both the **SP-2** and **MCH$^+$-2** states, a duration sufficient to collect current-voltage (I-V) curves while the molecule bridged the junction. The accumulation of 60 current-voltage curves of single **MCH$^+$-2** molecules are shown in Figure 4c. Two clear observation can be identified in the I–V plots. The first is that all the I-V curves are not symmetrical and that electric current rectification is evident with an average rectification ratio (RR) of 5 at ± 1 V. The second observation is that there are two sets of curves whose current rectification occur in opposite directions. We attribute these nearly inverse sets of I-V curves to the two opposite orientations that **MCH$^+$-2** can take in the junction (Figure 4d). These two orientations have the electron donor–bridge–acceptor axis in opposite directions yielding two different rectifying paths. Variation in values of the RRs within the I–V curves can be attributed to changes in dihedral angles about the C=C bond connecting the indoline and the chromene portions of the molecule. This would affect orbital overlap/conjugation between the donor (–OH) and acceptor (=N$^+$) units, and consequently alter the degree of rectification. Other reasons for the observed dispersion of RR involve changes to the molecule–electrode contact as well as changes in the orientation of the molecule within the junction.[38-39] It is worth noting here that, compared to the **MC**, protonation of the phenoxide anion to give the phenol (–OH) in **MCH$^+$-2** weakens the electron-donating ability of the phenolic moiety, which in turn can explain the moderate RR measured. We expect that a higher RR can be achieved with a zwitterionic-unprotonated **MC**, which has a larger dipole moment than that of the **MC-H$^+$** states, and which therefore has stronger donor–bridge–acceptor

character. For example, it was recently shown via large-scale molecular junctions that the current rectification correlates positively with the strength of the molecular dipole moment.[40] Values of RR increased from 20 to 200 when the molecular dipole moment changed from 2 D to 5 D [40]. A merocyanine rectifier can exceed these RR values because the dipole moment of the MC state can be made to reach 15-20 D.[16]

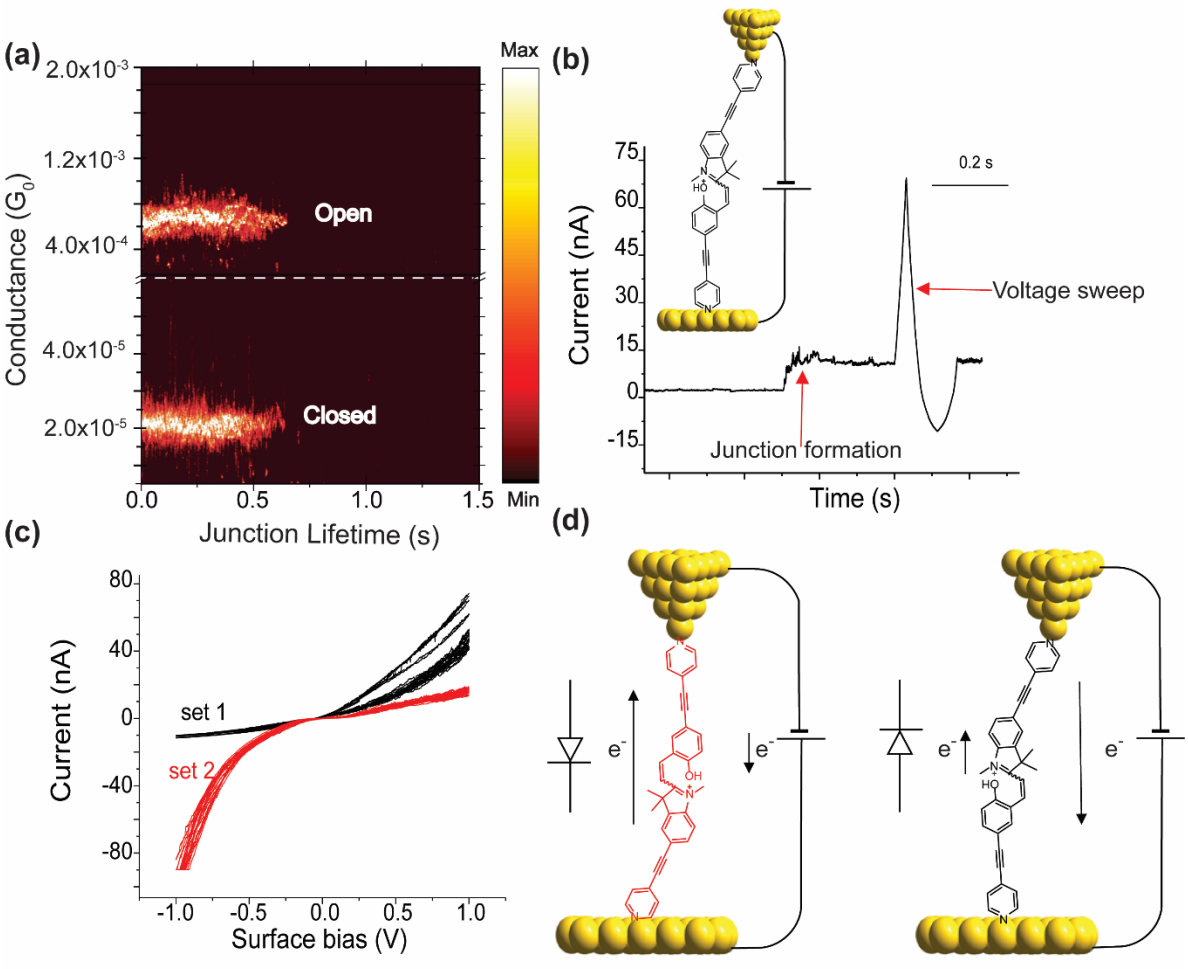

Figure 4. (a) STM-BJ blinking color maps to illustrate the conductance difference between **SP-2** (ring-closed) and **MCH$^+$-2** (ring-open) systems. The maps were obtained by accumulating 100 blinks and normalized to a common time origin. The average lifetime of the junctions is 0.5 s for both forms. Dotted line represents a switch to a higher current amplification for detecting the closed state. (b) Representative data for STM-BJ experiments where a voltage ramp is applied during a blink of a single-molecule Au–**MCH$^+$-2**–Au system. The current is monitored before and after the voltage sweep to ensure the voltage is ramped while the molecular junction is still intact. (c) Accumulation of 60 current–voltage curves measured during Au–**MCH$^+$-2**–Au blinks: 40% of the blinks showed a current–voltage features as depicted for set 1 (black traces), while the remaining 60% have features as for set 2 (red traces). (d) Depiction of the two possible orientations that **MCH$^+$-2** can adopt in a Au–**MCH$^+$-2**–Au junction, with the relative position of the ionized atoms in the molecule accounting for the opposite symmetry in the current rectification trends of panel (c).

2.3.3. Mechanical gating of conductance

Single-molecule conductance of the alkyne-terminated **SP-1** was measured using the tapping, current-stretching approach of STMBJ (Figure 5a).[32] Unlike the mostly flat and relatively smaller current plateaus observed in the current-stretching curves of **SP-2** (ca. 0.4 nm, Figure 3b), **SP-1** showed larger plateaus (ca. 0.8 nm, Figure 5b) with clear spikes or sudden jumps to a higher current level at the end of the stretching plateau in ca. 60% of the curves. Plateau-length histograms for **SP-1** and **SP-2** are shown in Figure S15 of the Supporting Information. We assign this unusual switching during stretching to the *in-situ* breakage of the spiro C–O bond during stretching. The resulting zwitterionic **MC-1** resulting from the spiro C–O cleavage leads to a higher conductance state due to the higher delocalization of the molecular orbitals in the open state compared to the completely broken conjugation in the closed state. The lifetime of the upper conductance level is short and happens only at the end of the plateaus. We assign the first long portion of the stretching (approximately flat plateaus up to 0.5-0.7 nm) to the bending of **SP-1** molecule in the junction from a relatively flat position to an upright position. Only after the molecule is in an upright position, mechanical strain on the molecular occurs leading to the rupture of the C–O bond. This consequently leads to a sudden jump in the current that is short-lived, after which the junction breaks as the tip continues its motion upward. The current jumps leads to a shoulder peak in the statistical histograms (Figure 5c and Figure S16, Supporting Information). The conductance peak at 8.0×10^{-5} G_0 is attributed to the closed **SP-1** state and the peak at 3.7×10^{-4} G_0 is attributed to the open **MC-1** state that occurs during the pulling stage (Figure 5c). Of a particular note is the sudden jump in the current when pulling **SP-1** as opposed to the gradual change in current previously reported.[41-43] For example, Tao and co-workers have reported a gradual increase in the current when stretching a 1,4 benzenedithiol junction.[42] The current change was attributed to a strain-induced shift of the highest occupied molecular orbital towards the Fermi level of the electrodes.[42] Other

observations include a gradual decrease in the current as the junction is pulled away reported by Haiss et al.[41] in which the current showed a dependence on the tilt-angle of the molecular junction with respect to the electrodes. The sudden switching to a higher conductance state in **SP-1**/**MC-1** system therefore indicates the breakage of the C–O spiro-bond during stretching rather than a shift of molecular orbitals towards the gold Fermi level.

MC-1 is zwitterionic with a large dipole moment which is expected to behave as a diode with a large RR. However, the **MC-1** is only induced during pulling of the junction and therefore during motion of the STM tip which makes it not possible to measure the I-V properties in steady state. Measuring the I-V properties of the MC state can be possibly achieved by designing molecules with electron withdrawing NO_2 groups on the chromene side of the molecules. When irradiated with UV light, these molecules will likely exhibit a slow reverse switching back to the SP. This is because the electron withdrawing NO_2 groups will remove electron density from the phenoxide anion of the MC state, slow the cyclization back to the SP state and therefore will facilitate the measurements on the MC state.

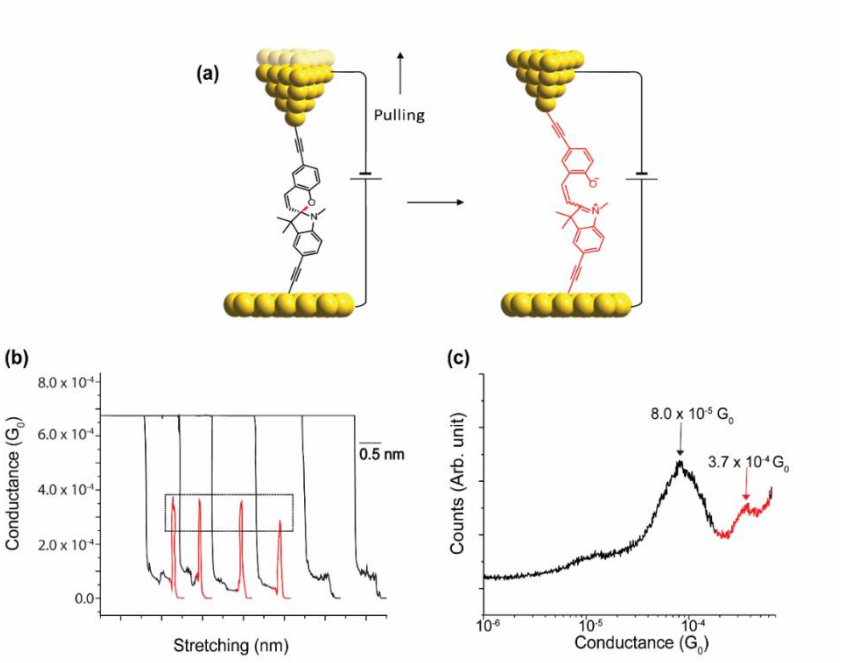

Figure 5. a) Schematic describing the stretching of a single **SP-1** molecule in a STM-BJ experiment. (b) Representative current–distance curves of **SP-1**. The switching to a higher conductance level occur in 60% of the collected current–stretching curves. (c) Conductance histograms of **SP-1** (black line), with the higher conducting **MC-1** state appearing as a shoulder peak (red portion of the trace).

3. CONCLUSIONS

In summary, we have demonstrated the operation of a single-molecule electrical switch, based on chemical and mechanical stimulation of spiropyrans, with an on/off conductance ratio of one order of magnitude. In one case (**SP-2**) switching is effected by ring-opening of the spiropyran to the open protonated merocyanine (**MCH$^+$-2**) state and can be reversibly controlled by acid/base stimuli. The protonated merocyanine is a current rectifier with an average rectification ratio of 5 at ± 1V. Current rectification is due to the attachment of the electron deficient side of the molecule to the negative terminal of the circuit. In the second case (**SP-1**), switching between the closed-resistive (**SP**) and open-conductive (**MC**) states is achieved through tensile strain. This is possible because of the strong Au–C bonds to the electrodes.

4. EXPERIMENTAL SECTION

4.1. SAM formation and electrochemical measurements

The electrochemical measurements were performed with a CHI650 (CH Instruments, USA) electrochemical workstation and a conventional three-electrode system with a platinum wire as the auxiliary electrode. An Ag/AgCl aqueous electrode (1M KCl, CH Instruments, USA) served as the reference and Au (111) single crystal modified with an **SP-1** monolayer, used as the working electrode. The measurements were performed in 0.1 M $NaClO_4$ as the electrolyte. Single-crystal Au (111) disks were first cleaned in a hot Piranha solution for 3 min (3:1 (v/v) mixture of concentrated sulfuric acid to 30 wt % hydrogen peroxide), rinsed with Milli-QTM water and then annealed using a hydrogen flame. Annealed crystals were cooled down to room temperature, washed with Milli-Q^{TM} water, dichloromethane and then blown dry under stream of argon gas. The crystals were then transferred to a 5 mM solution of **SP-1** in dichloromethane.

The electrodes were sealed and left standing overnight before performing the "click" reaction with azidomethyl ferrocene.

"Click" reaction: to a reaction vial containing the **SP-1**-functionalized Au (111) surface were added (i) azidomethyl-ferrocene (10 mM, ethanol/water, 2 : 1), (ii) copper(II) sulfate pentahydrate (0.8 mol% relative to the azide) and (iii) sodium ascorbate (80 mol% relative to the azide). The reaction was stopped after 1 h and rinsed consecutively with copious amounts of water and ethanol before being analyzed. The density of electroactive ferrocene probes on the electrode surface was determined by integrating the area under the oxidation and reduction waves in cyclic voltammetry.

4.2. Single-molecule STM break junction

STM experiments were carried out with PicoSPM 1 microscope head controlled by a "Picoscan 2,500 electronics, from Agilent". The STM-BJ data were collected using an NI-DAQmx/BNC-2,110 national instruments (LabVIEW data collection system) and analysed with code based on LabVIEW software. In the blinking approach, the tunnelling current is first stabilized for 1 h until tunnelling current variation of < 10 % is obtained. Current transients are then captured when a molecule connect between the STM tip and the surface in the presence of 4 μM solution (mesitylene/dicholoromethane solvent mixture (10:1 v/v)) of **SP-1** and **SP-2**. When needed, **SP-2** was switched to the **MCH$^+$-2** state by the addition of two equivalents of TFA. **MCH$^+$-2** was reverted back to **SP-2** by the addition of the neutralizing base, TEA. In the tapping-mode approach (current vs. distance approach), the STM tip is moved in and out from a surface in the presence of 4 μM solution (mesitylene/dicholoromethane solvent mixture (10:1 v/v)) of the molecules. 10,000 of current versus distance curves are collected and accumulated in conductance histogram. Curves displaying clear plateaus that evidence the formation of a single-molecule bridge were selected and used to build the conductance histograms. An

automatic selection driven by a home-made Labview code was used to select the individual traces. The histograms were made by applying the same automated selection criteria to each set of recorded decay curves. The percentage decay curves that showed clear plateaus displaying the occurrence of a single molecule bridge were typically 20–35 % and were all selected to build the histograms. This selection process made peaks in the conductance histograms more prominent above the tunnelling background.

ASSOCIATED CONTENT

Information

Detailed synthetic methods of molecules **SP-1** and **SP-2,** and sections of characterization (Crystal structures with CCDC numbers 1862693 and 1923329 for **3** and **SP-1**, NMR, cyclic voltammetry,UV-Vis, XPS and STM-BJ data) are included in the Supporting Information. The Supporting Information is available free of charge on the ACS Publications website.

AUTHOR INFORMATION

The authors declare no competing financial interest

Corresponding Authors

nadim.darwish@curtin.edu.au

matthew.piggott@uwa.edu.au

george.koutsantonis@uwa.edu.au

Author Contributions

M.C.W. and C.R.P. contributed equally to this work. N.D. performed the single-molecule measurements and analysed the data. C.R.P., N.D. and R.B.D. performed the surface characterization, UV-Vis spectroscopy and the electrochemical measurements and analysed the data. M.C.W., G.A.K., M.J.P., D.J., T.P., B.W.S. and A.S. designed and synthesized **SP-1**

and **SP-2** compounds and performed the synthetic characterization. S.C. synthesized the azidomethyl-ferrocene and performed the XPS measurements. N.D. wrote the manuscript with contributions from all authors. All authors read, discussed the results and commented on the manuscript.

ACKNOWLEDGMENT

N.D. and S.C. thanks the Australian Research Council for DE160101101, DE160100732 and DP190100735 grants. This research was partially supported by the Australian Government through the Australian Research Council's Discovery Projects funding scheme (project DP150104117).

REFERENCES

(1) Sun, L.; Diaz-Fernandez, Y. A.; Gschneidtner, T. A.; Westerlund, F.; Lara-Avila, S.; Moth-Poulsen, K., Single-Molecule Electronics: from Chemical Design to Functional Devices. *Chem. Soc. Rev.* **2014,** *43* (21), 7378-7411.

(2) Lo, W. Y.; Zhang, N.; Cai, Z.; Li, L.; Yu, L., Beyond Molecular Wires: Design Molecular Electronic Functions Based on Dipolar Effect. *Acc. Chem. Res.* **2016,** *49* (9), 1852-1863.

(3) Darwish, N.; Paddon-Row, M. N.; Gooding, J. J., Surface-Bound Norbornylogous Bridges as Molecular Rulers for Investigating Interfacial Electrochemistry and as Single Molecule Switches. *Acc. Chem. Res.* **2013,** *47* (2), 385-395.

(4) Tao, N. J., Electron Transport in Molecular Junctions. *Nat. Nanotechnol.* **2006,** *1* (3), 173-181.

(5) Ratner, M., A Brief History of Molecular Electronics. *Nat. Nanotechnol.* **2013,** *8* (6), 378-381.

(6) Darwish, N.; Díez-Pérez, I.; Da Silva, P.; Tao, N.; Gooding, J. J.; Paddon-Row, M. N., Observation of Electrochemically Controlled Quantum Interference in a Single Anthraquinone-Based Norbornylogous Bridge Molecule. *Angew. Chem., Int. Ed.* **2012,** *51* (13), 3203-3206.

(7) Darwish, N.; Díez-Pérez, I.; Guo, S.; Tao, N.; Gooding, J. J.; Paddon-Row, M. N., Single Molecular Switches: Electrochemical Gating of a Single Anthraquinone-Based Norbornylogous Bridge Molecule. *J. Phys. Chem. C.* **2012,** *116* (39), 21093-21097.

(8) Darwish, N.; Aragonès, A. C.; Darwish, T.; Ciampi, S.; Diez-Perez, I., Multi-Responsive Photo-and Chemo-Electrical Single-Molecule Switches. *Nano Lett.* **2014,** *14* (12), 7064-7070.
(9) Gerhard, L.; Edelmann, K.; Homberg, J.; Valášek, M.; Bahoosh, S. G.; Lukas, M.; Pauly, F.; Mayor, M.; Wulfhekel, W., An Electrically Actuated Molecular Toggle Witch. *Nat. Commun.* **2017,** *8*, 14672.
(10) Cai, S.; Deng, W.; Huang, F.; Chen, L.; Tang, C.; He, W.; Long, S.; Li, R.; Tan, Z.; Liu, J., Light-Driven Reversible Intermolecular Proton Transfer at Single-Molecule Junctions. *Angew. Chem.* **2019,** *131* (12), 3869-3873.
(11) Jan van der Molen, S.; Liljeroth, P., Charge Transport Through Molecular Switches. *J. Phys.: Condens. Matter*. **2010,** *22* (13), 133001.
(12) Lörtscher, E.; Gotsmann, B.; Lee, Y.; Yu, L.; Rettner, C.; Riel, H., Transport Properties of a Single-Molecule Diode. *ACS Nano.* **2012,** *6* (6), 4931-4939.
(13) Roldan, D.; Kaliginedi, V.; Cobo, S.; Kolivoska, V.; Bucher, C.; Hong, W.; Royal, G.; Wandlowski, T., Charge Transport in Photoswitchable Dimethyldihydropyrene-Type Single-Molecule Junctions. *J. Am. Chem. Soc.* **2013,** *135* (16), 5974-5977.
(14) Zhang, J. L.; Zhong, J. Q.; Lin, J. D.; Hu, W. P.; Wu, K.; Xu, G. Q.; Wee, A. T. S.; Chen, W., Towards Single Molecule Switches. *Chem. Soc. Rev.* **2015,** *44* (10), 2998-3022.
(15) Minkin, V. I., Photo-, Thermo-, Solvato-, and Electrochromic Spiroheterocyclic Compounds. *Chem. Rev.* **2004,** *104* (5), 2751-2776.
(16) Klajn, R., Spiropyran-Based Dynamic Materials. *Chem. Soc. Rev.* **2014,** *43* (1), 148-184.
(17) Darwish, T. A.; Evans, R. A.; James, M.; Malic, N.; Triani, G.; Hanley, T. L., CO_2 Triggering and Controlling Orthogonally Multiresponsive Photochromic Systems. *J. Am. Chem. Soc.* **2010,** *132* (31), 10748-10755.
(18) Bahr, J. L.; Kodis, G.; de la Garza, L.; Lin, S.; Moore, A. L.; Moore, T. A.; Gust, D., Photoswitched Singlet Energy Transfer in a Porphyrin-Spiropyran Dyad. *J. Am. Chem. Soc.* **2001,** *123* (29), 7124-7133.
(19) Aviram, A.; Ratner, M. A., Molecular Rectifiers. *Angew. Chem.* **1974,** *29* (2), 277-283.
(20) Davis, D. A.; Hamilton, A.; Yang, J.; Cremar, L. D.; Van Gough, D.; Potisek, S. L.; Ong, M. T.; Braun, P. V.; Martínez, T. J.; White, S. R., Force-Induced Activation of Covalent Bonds in Mechanoresponsive Polymeric Materials. *Nature.* **2009,** *459* (7243), 68-72.
(21) Marevtsev, V.; Zaichenko, N., Peculiarities of Photochromic Behaviour of Spiropyrans and Spirooxazines. *J. Photochem. Photobiol., A.* **1997,** *104* (1-3), 197-202.

(22) Bejarano, F.; Olavarria-Contreras, I. J.; Droghetti, A.; Rungger, I.; Rudnev, A.; Gutiérrez, D.; Mas-Torrent, M.; Veciana, J.; van der Zant, H. S. J.; Rovira, C.; Burzurí, E.; Crivillers, N., Robust Organic Radical Molecular Junctions Using Acetylene Terminated Groups for C–Au Bond Formation. *J. Am. Chem. Soc.* **2018,** *140* (5), 1691-1696.

(23) Lee, C. K.; Davis, D. A.; White, S. R.; Moore, J. S.; Sottos, N. R.; Braun, P. V., Force-Induced Redistribution of a Chemical Equilibrium. *J. Am. Chem. Soc.* **2010,** *132* (45), 16107-16111.

(24) Lukyanov, B.; Lukyanova, M., Spiropyrans: Synthesis, Properties, and Application. *Chem. Heterocycl. Compd.* **2005,** *41* (3), 281-311.

(25) Walkey, M. C.; Byrne, L. T.; Piggott, M. J.; Low, P. J.; Koutsantonis, G. A., Enhanced Bi-Stability in a Ruthenium Alkynyl Spiropyran Complex. *Dalton Trans.* **2015,** *44* (19), 8812-8815.

(26) Sonogashira, K., Development of Pd–Cu Catalyzed Cross-Coupling of Terminal Acetylenes with sp2-Carbon Halides. *J. Organomet. Chem.* **2002,** *653* (1-2), 46-49.

(27) Trasobares, J.; Vuillaume, D.; Théron, D.; Clément, N., A 17 GHz Molecular Rectifier. *Nat. Commun.* **2016,** *7*, 12850.

(28) Han, S. W.; Seo, H.; Chung, Y. K.; Kim, K., Electrochemical and Vibrational Spectroscopic Characterization of Self-Assembled Monolayers of 1, 1 '-Disubstituted Ferrocene Derivatives on Gold. *Langmuir.* **2000,** *16* (24), 9493-9500.

(29) Gooding, J. J.; Ciampi, S., The Molecular Level Modification of Surfaces: from Self-Assembled Monolayers to Complex Molecular Assemblies. *Chem. Soc. Rev.* **2011,** *40* (5), 2704-2718.

(30) Singh, A.; Chowdhury, D. R.; Paul, A., A Kinetic Study of Ferrocenium Cation Decomposition Utilizing an Integrated Electrochemical Methodology Composed of Cyclic Voltammetry and Amperometry. *Analyst.* **2014,** *139* (22), 5747-5754.

(31) Wojtyk, J. T. C.; Wasey, A.; Xiao, N.-N.; Kazmaier, P. M.; Hoz, S.; Yu, C.; Lemieux, R. P.; Buncel, E., Elucidating the Mechanisms of Acidochromic Spiropyran-Merocyanine Interconversion. *J. Phys. Chem. A.* **2007,** *111* (13), 2511-2516.

(32) Xu, B.; Xiao, X.; Tao, N. J., Measurements of Single-Molecule Electromechanical Properties. *J. Am. Chem. Soc.* **2003,** *125* (52), 16164-16165.

(33) Xu, B.; Tao, N. J., Measurement of Single-Molecule Resistance by Repeated Formation of Molecular Junctions. *Science.* **2003,** *301* (5637), 1221-1223.

(34) Zhang, L.; Laborda, E.; Darwish, N.; Noble, B. B.; Tyrell, J. H.; Pluczyk, S.; Le Brun, A. P.; Wallace, G. G.; Gonzalez, J.; Coote, M. L.; Ciampi, S., Electrochemical and Electrostatic Cleavage of Alkoxyamines. *J. Am. Chem. Soc.* **2018,** *140* (2), 766-774.

(35) Aragonès, A. C.; Haworth, N. L.; Darwish, N.; Ciampi, S.; Bloomfield, N. J.; Wallace, G. G.; Diez-Perez, I.; Coote, M. L., Electrostatic Catalysis of a Diels–Alder Reaction. *Nature.* **2016,** *531* (7592), 88-91.

(36) Nichols, R. J.; Higgins, S. J., Molecular Junctions: Single-Molecule Contacts Exposed. *Nat. Mater.* **2015,** *14* (5), 465-466.

(37) Nichols, R. J.; Haiss, W.; Higgins, S. J.; Leary, E.; Martin, S.; Bethell, D., The Experimental Determination of the Conductance of Single Molecules. *Phys. Chem. Chem. Phys.* **2010,** *12* (12), 2801-2815.

(38) Rascón-Ramos, H.; Artés, J. M.; Li, Y.; Hihath, J., Binding Configurations and Intramolecular Strain in Single-Molecule Devices. *Nat. Mater.* **2015,** *14*, 517-522.

(39) Diez-Perez, I.; Hihath, J.; Hines, T.; Wang, Z. S.; Zhou, G.; Müllen, K.; Tao, N., Controlling Single-Molecule Conductance Through Lateral Coupling of π Orbitals. *Nat. Nanotechnol.* **2011,** *6*, 226-231.

(40) Lamport, Z. A.; Broadnax, A. D.; Harrison, D.; Barth, K. J.; Mendenhall, L.; Hamilton, C. T.; Guthold, M.; Thonhauser, T.; Welker, M. E.; Jurchescu, O. D., Fluorinated Benzalkylsilane Molecular Rectifiers. *Sci. Rep.* **2016,** *6*, 38092.

(41) Haiss, W.; Wang, C.; Grace, I.; Batsanov, A. S.; Schiffrin, D. J.; Higgins, S. J.; Bryce, M. R.; Lambert, C. J.; Nichols, R. J., Precision Control of Single-Molecule Electrical Junctions. *Nat. Mater.* **2006,** *5* (12), 995-1002.

(42) Bruot, C.; Hihath, J.; Tao, N., Mechanically Controlled Molecular Orbital Alignment in Single Molecule Junctions. *Nat. Nanotechnol*. **2011,** *7*, 35-40.

(43) Reecht, G.; Bulou, H.; Scheurer, F.; Speisser, V.; Mathevet, F.; González, C.; Dappe, Y. J.; Schull, G., Pulling and Stretching a Molecular Wire to Tune its Conductance. *J. Phys. Chem. Lett.* **2015,** *6* (15), 2987-2992.

Table of contents graphic